

THE UNUSUAL INFRARED COLORS OF A FAINT OBJECT IN THE CHAMAELEON I STAR-FORMING REGION¹

F. COMERÓN

European Southern Observatory, Karl-Schwarzschild-Strasse 2, D-85748 Garching bei München, Germany; fcomeron@eso.org

AND

P. CLAES

European Space Agency, ESTEC/APP-NSG, NL-2200 AG Noordwijk, Netherlands; pclaes@estec.esa.int

Received 2003 September 5; accepted 2003 October 23

ABSTRACT

We present deep near-infrared ($J_S HK_S$) imaging observations, carried out with the ESO Very Large Telescope (VLT), of a field in the Chamaeleon I star forming region in an attempt to identify possible members with masses comparable to, or below, the mass of Jupiter. We focus on an object, Cha I J110814.2–773649, which stands out as an outlier in color-color and color-magnitude diagrams of the field, with $H = 22.16_{-0.17}^{+0.21}$, $H-K_S = -0.01_{-0.24}^{+0.26}$, and $J_S-H = 2.00_{-0.62}^{+\infty}$. H -band spectroscopy of this object shows that the unusual colors are not due to emission lines in the region; furthermore, this spectroscopy allows clear detection of the object's continuum. Assuming membership in Chamaeleon I and an age of 2 Myr (the age of most members of Cha I), the blue $H-K_S$ color and the absolute magnitude are consistent with model predictions for a cool, sub-Jupiter mass object with strong dust depletion in the atmosphere. However, the very red J_S-H color implied by the marginal detection in the J_S band is unexpected in an object with such atmospheric properties. We speculate that this might be due to differences in the properties of dust and its depletion under the photosphere with respect to field objects (T dwarfs) that have a similar temperature, these differences resulting from both the youth and the low surface gravity of a low-mass member of a star-forming region. We also consider the alternative possibility that Cha I J110814.2–773649 might actually be a high-redshift object, whose red J_S-H color could result from absorption of the flux blueward of $\text{Ly}\alpha$ in the J band. We find that this possibility would be marginally compatible with the $J_S HK_S$ photometry of Cha I J110814.2–773649 if it were an unreddened starburst at $8.5 < z < 11$.

Subject headings: stars: formation — stars: low-mass, brown dwarfs

1. INTRODUCTION

The search for the bottom of the stellar mass function, one of the main goals of surveys of star-forming regions just less than a decade ago (Tinney 1995), has now been replaced by the search for objects beyond the bottom of the brown dwarf mass function, and for the ultimate limit below which compact objects cannot form in isolation. The realization that freely floating objects continue to be found as surveys probe lower and lower masses (Zapatero Osorio et al. 1999, 2000, 2002; Martín & Zapatero Osorio 2003; Lucas & Roche 2000; Lucas et al. 2001) has prompted a reconsideration of object formation theories (Reipurth & Clarke 2001; Boss 2001) and even of the basic definitions and nomenclature that apply to objects not orbiting a larger body and whose mass is near or below the deuterium-burning limit of $\simeq 12$ Jupiter masses (M_J) (Saumon et al. 1996). Despite recent progress, the direct detection of truly Jupiter mass and even lighter objects outside our solar system remains an observational challenge pushing current instrumental capabilities to their limits.

The complex molecular and dust chemistry in the atmospheres of objects with temperatures near $T \sim 1000$ K causes major flux redistributions that increase the near-infrared brightness with respect to blackbodies by orders of magnitude, and produce highly peculiar colors that are difficult to mistake

for any other astrophysical objects (Burrows et al. 1997). These two properties suggest that such cool objects may be relatively easy to detect thanks to their brightness, and to recognize thanks to their colors. Actual observations of objects with spectral type T (Kirkpatrick et al. 1999), brown dwarfs much cooler than the coolest stars, confirm the main results of theoretical modeling (Burgasser et al. 1999; Leggett et al. 2000; Chabrier et al. 2000; Burrows et al. 2001; Dahn et al. 2002). The large age difference between millions of years old star-forming regions and the billions of years old field population implies dramatic differences between the masses of newly formed and evolved T dwarf-like objects: while a brown dwarf of $40M_J$ reaches a temperature of $\simeq 1200$ K (which marks the approximate boundary between L and T dwarfs; Burgasser et al. 2002) at the age of 1 Gyr, the same temperature corresponds to a mass of around $5M_J$ at the age of 10 Myr, and to a mass of less than $2M_J$ at 1 Myr (Baraffe et al. 2003). The near-infrared luminosities predicted by models indicate that T dwarf-like objects in the nearest star-forming regions should be within the reach of current instrumentation in 4–8 m class telescopes, as confirmed by the recent discovery of a possible member of the σ Ori aggregate with T dwarf-like spectral features (Zapatero Osorio et al. 2002). However, the faint magnitudes necessary for such observations extends the horizon to high- z objects with appearances very different from those of objects in the local universe, thus requiring extra care in the interpretation of objects with unusual colors.

This paper presents observations, carried out with the ESO Very Large Telescope (VLT), of a very faint object in the

¹ Based on observations obtained at the European Southern Observatory using the Very Large Telescope, Cerro Paranal, Chile (programmes 64.L-0049[A] and 67.C-0109[B]).

direction of the Cha I star-forming region with highly unusual infrared colors characterized by a blue $H-K_S$ index combined with a very red J_S-H index. Spectroscopy demonstrates that these colors are due to a continuum spectrum, and not to the presence of emission lines in the H band. We hypothesize that the object might be a very low mass member of Cha I, whose faintness would then suggest an extremely low, possibly sub-Jupiter mass that would make it the least massive compact object detected so far outside the solar system. However, we also contemplate the possibility that the object might be an extremely high- z object, as we find marginal consistency between its colors and those expected from an unobscured starburst at a redshift $z > 8.5$ that would make it a J -band dropout.

2. OBSERVATIONS AND DATA REDUCTION

The Chamaeleon I cloud, at 160 pc from the Sun (Wichmann et al. 1998), is one of the nearest star-forming regions. Besides its proximity, other factors make it an attractive target for the study of its lowest mass contents: the low internal extinction over most of its subtended area yields a mostly unobscured view of its contents, and its moderately high galactic latitude (18° south of the Galactic plane) decreases the density of background sources. Moreover, several very low mass stellar and substellar members have been already detected there with masses down to $20-30M_J$ (Comerón, Neuhäuser, & Kaas 2000; Comerón et al. 2003), thus encouraging the search for even lower mass objects.

2.1. Imaging

We obtained deep imaging in the J_S , H , and K_S bands of a field covering 2.5×2.5 on the sky using the Infrared Spectrometer And Array Camera (ISAAC) at the VLT, on the nights of 2000 March 27 and 28. The field is centered at $\alpha(2000) = 11^{\text{h}}08^{\text{m}}16^{\text{s}}.5$, $\delta(2000) = -77^\circ 35' 36''$, and was chosen because of the existence of previously identified brown dwarf candidates in its proximity (Comerón et al. 2000); the field also avoids regions of high extinction and bright nearby stars that might produce ghost images on the detector.

We obtained the images by integrating on the field for approximately 30 minutes in a given filter, splitting the integration into several individual exposures obtained with telescope offsets of a few tens of arcseconds. We then switched to a different filter and repeated the procedure. We distributed the observations in each of the three filters along our two observing nights to average over time any possible source variability with timescales shorter than the span of our observing run. Each block of integrations in each filter was combined into a single image, in which the individual frames were reduced by subtracting a sky frame (constructed by taking the median average of the field frames, uncorrected for telescope offsets, so as to remove the source images and cosmic-ray hits) and dividing by a master flat field based on sequences of twilight-sky exposures with different illumination levels. All the blocks in each filter were then combined into a deep image of the field, by means of an average in which the contribution of each individual block was weighted with the inverse square of the dispersion of the counts of its background. In this way, “noisy” frames obtained with relatively high background levels had a reduced contribution to the average. Total exposure times were 2.7 hr in J_S , 2.5 hr in H , and 7.9 hr in K_S . The longer exposure times in K_S are due to the blue $H-K_S$ indices expected for the objects of interest in this work.

The targeted region does not show any obvious nebulosity in the visible and, given the progressively lower efficiency of scattering by small dust grains toward longer wavelengths, the visibility of any possible remaining faint nebulosity at infrared wavelengths is expected to be even lower. Indeed, tenuous filamentary nebulosity across the field is perceptible only in the final combined images, most clearly in the J_S image. The sky frame constructed according to the procedure described above effectively filters out extended uniform nebulosity, as well as point sources and small extended sources. However, it would leave unfiltered any nebulosity with brightness variations over angular scales comparable to the amplitude of the offset pattern, which would then be apparent in the sky-subtracted frames as zones with local negative backgrounds, and may thus bias the flux estimates of the detected sources. No such effect is seen at all in our images, thus giving us confidence that the sky-subtraction procedure followed is well suited for the reduction of our target field.

Photometric calibration was performed at the beginning of each night by observing the standard star S064-F, lying near the Cha I region, followed by an observation of the target field at a nearly identical air mass. This standard is a part of the set that defines the Las Campanas/Palomar Near-Infrared Camera and Multi-Object Spectrometer (NICMOS) system (Persson et al. 1998), which the broadband filter plus detector system of ISAAC matches well. This allowed us to establish a network of local secondary standards, which were used to determine the photometric zero-points of the deep images. We then stacked together the three deep frames in each filter, and used the DAOFIND task of the DAOPHOT package (Stetson 1987), available in IRAF,² for automated source detection. Photometry was performed by point-spread function (PSF) fitting, using the brightest point sources in the field as a reference for PSF determination with the DAOPHOT PEAK task. After experimenting with different PSF functional forms available within the DAOPARS package, we chose a PSF consisting of a Gaussian analytical part plus a lookup table of residuals, both constant across the field. Comparison with results obtained using other forms for the analytical component showed no major differences in the results. The measured FWHM of the PSF in the combined images is $0''.81$ (J_S), $0''.71$ (H), and $0''.66$ (K_S). Since the photometry was performed by fitting of a stellar PSF it is accurate only for point sources, which are the objects of interest in this work. Photometric errors and detection limits for point sources were derived by adding artificial stars (constructed by scaling the derived PSF according to the desired magnitude) to the frames, and then recovering their photometry in the same way as for the real stars. The errors thus measured correspond to the 1σ scatter in the input magnitudes of the artificial stars of a given recovered magnitude. We obtained an average of 5σ detection limits for point sources of $J_S = 23.20$, $H = 22.30$, and $K_S = 22.35$, with slight regional variations below the 0.1 mag level, due to the presence of faint filamentary nebulosity across the field.

Figure 1 shows the $(H-K_S, H)$ color-magnitude diagram of all the sources detected in our images that have a detection above the 3σ level in at least one of the bands. At the bright end ($H < 18$) late-type stars, with a narrow range of colors and a well defined blue boundary at $H-K_S \simeq 0.3$, dominate. Both the narrowness of the range and the low value of the

² IRAF is distributed by NOAO, which is operated by the Association of Universities for Research in Astronomy, Inc., under contract to the National Science Foundation.

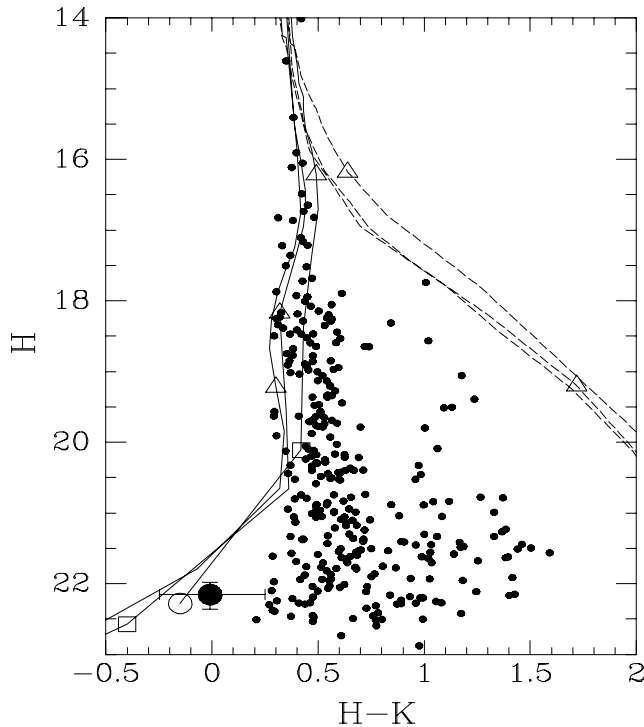


FIG. 1.— $(H-K_S, H)$ color-magnitude diagram of the objects detected in our images. Only objects exceeding a detection threshold of 5σ in our H -band images are plotted. Cha I J110814.2–773649 is the point at the bottom left with error bars plotted on it. The lines are theoretical isochrones for ages 1, 5, and 10 Myr according to two different sets of models (see § 3.2.2) at the distance of Chamaeleon I. The dashed lines correspond to the DUSTY models of Chabrier et al. (2000), in which dust grains form and stay in the atmosphere. The solid lines correspond to the COND models (Baraffe et al. 2003), in which dust grains precipitate under the photosphere as soon as they are formed. The latter set of models is expected to better represent the cool ($T \sim 1000$ K) objects of interest in this work. The symbols plotted on the lines denote the position of objects of different masses at the age of each isochrone: triangles correspond to $5M_\odot$; squares, $1M_\odot$; and circles, $0.5M_\odot$. The large overlap among the isochrones corresponding to each model implies a large degeneracy between age and mass. The red, bright object near the dashed lines at $H = 17.74$ and $H-K_S = 1.01$ is not a candidate L dwarf, but a well-resolved elliptical galaxy

$H-K_S$ index show that extinction is low and fairly uniform throughout the region. This is confirmed by the color-color magnitude diagram (Fig. 2), where most objects cluster at the colors expected for mid-to-late type stellar photospheres reddened by extinctions between 0.2 and 0.6 mag at K_S .

At fainter magnitudes extragalactic sources, generally redder and often resolved, progressively take over. However, there is an obvious outlier at $H-K_S = -0.01^{+0.26}_{-0.24}$, $H = 22.16^{+0.21}_{-0.17}$. The object (hereafter referred to as Cha I J110814.2–773649 after its J2000 equatorial coordinates) is at most barely detected at $J_S \simeq 24.16^{+\infty}_{-0.59}$, implying $J_S-H = 2.00^{+\infty}_{-0.62}$.

Even though measurement uncertainties are marginally compatible with a $(H-K_S)$ color close to the blue boundary defined by the other sources in the field, this color's combination with the high upper limit in (J_S-H) implies very unusual near-infrared colors for Cha I J110814.2–773649. This is more clearly visible in Figure 2, where the separation of Cha I J110814.2–773649 with respect to all the other objects in the field is very clear. No other objects with comparable photometric properties are detected in the field. Figure 3 shows a small section of the field centered on Cha I J110814.2–773649

in the three bands used. The fact that it is clearly seen at H but hardly at all at J_S would suggest a considerable brightness at K_S , but, as can be seen by comparison with the objects surrounding it, this does not happen. A comparison with the radial plots of the PSF reference stars does not show any evidence that Cha I J110814.2–773649 is spatially extended.

2.2. Spectroscopy

The photometric properties of Cha I J110814.2–773649 are highly unusual for an object with a continuum-dominated spectrum, but they might be reproduced by an active galactic nucleus (AGN) or QSO with intense emission lines conveniently redshifted (vanden Berk et al. 2001): one or a few strong lines in the H band would make the object appear red in J_S-H and blue in $H-K_S$. Obvious candidates are $H\alpha$ redshifted to $z \simeq 1.5$, $H\beta+[O\text{ III}]$ redshifted to $z \simeq 2.3$, or $[O\text{ II}]$ redshifted to $z \simeq 3.4$.

We obtained a 10 hr H -band spectrum of Cha I J110814.2–773649, also using ISAAC at the VLT, on the nights of 2001 April 29 and 2001 May 1. The goal was to determine if emission lines dominated the H -band flux of the object (which should be relatively straightforward to detect in such a deep spectrum) or, alternatively, if an unusual continuum spectral energy distribution existed (which should result in nondetection of the object, or a marginal detection at most, due to the spread of the flux over the spectral range covered). We were fortunate to enjoy excellent transparency conditions and subarcsecond seeing during virtually the entire time devoted to these observations.

Individual spectra were obtained with the $1''0$ slit oriented to include a brighter, $H = 16.83$ reference star located $16''$ from Cha I J110814.2–773649. A total of 200 individual

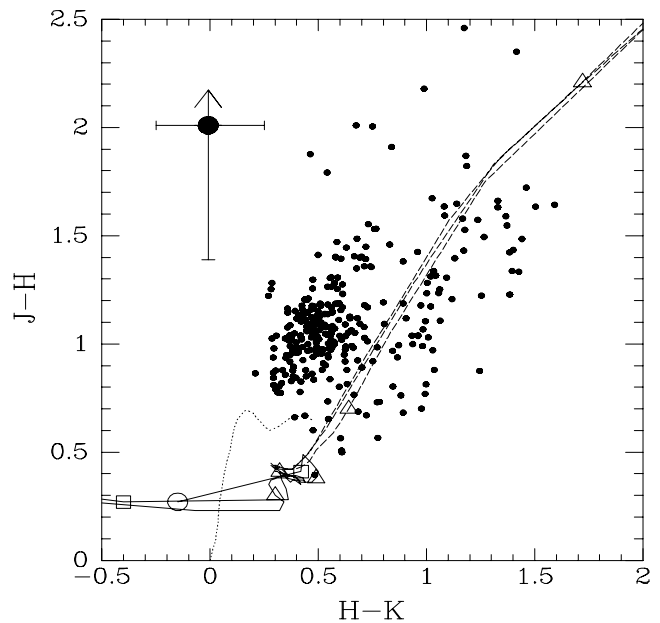


FIG. 2.— $(H-K_S, J_S-H)$ diagram of all objects having H -band detections at a level higher than 5σ in our images. Cha I J110814.2–773649 is the point at the upper left with error bars plotted on it. The solid and dashed lines, and the open symbols along them, represent theoretical isochrones as in Fig. 1. The dotted line is the locus of dwarf stars between spectral types B and M6, from Bessell & Brett (1988). The displacement between the highest density of points in the diagram, which corresponds to stars in the background of the Cha I cloud, and this locus is due to the moderate extinction caused by the dust in the star-forming region that pervades the imaged area.

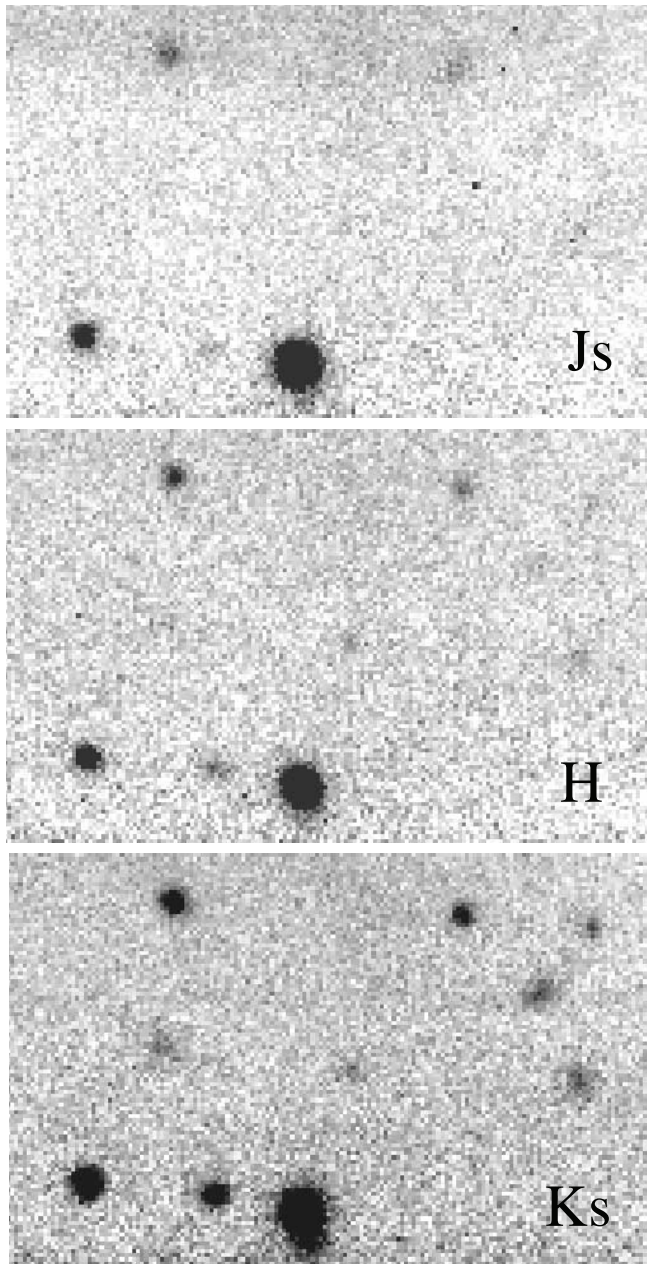


FIG. 3.—Images of Cha I J110814.2–773649 in the J_s , H , and K_s bands. This is a small portion ($23'' \times 15''$) of the field imaged in our observations. Cha I J110814.2–773649 is the faint object in the center of the images.

spectra of 180 s of exposure time each were obtained with nodding along the slit combined with a small random offset around each of the two nod positions. The presence of the reference star provides an easy way to monitor the object centering during the integrations and to correct for telescope nodding at the reduction stage; it also includes a secondary calibrator for telluric absorption correction in each frame. Consecutive frames taken at two different nod positions were subtracted to cancel sky (emission) lines, and then divided by a spectroscopic flat field frame constructed from calibration frames taken with an internal continuum lamp switched on and off. We subsequently refer to these sky-subtracted, flat-fielded frames as “pairwise-subtracted frames.”

At the time our observations were obtained, ISAAC suffered from a pickup noise problem that imposed a wave pattern

along detector columns, corresponding to the spatial direction. The amplitude of the pattern is far too low to be seen in the individual pairwise-subtracted frames, where it is hidden by the background and readout noise. However, it becomes readily apparent at the very high sensitivity levels obtained when co-adding the 200 pairwise-subtracted frames after correcting for the telescope nodding using the trace of the spectrum of the bright star as a reference. We removed this pattern by adopting an additional step in the data reduction, which consisted of subtracting from each pairwise-subtracted frame another frame containing the wave pattern almost uniquely. To do this, we took advantage of the fact that the wavelength of the pickup noise pattern was almost exactly 6.5 pixels along the spatial direction. We thus produced a wave-pattern frame by combining and median-filtering the pairwise-subtracted frame with copies of itself shifted respectively by 13, 26, 39, 52, 65, and 78 pixels along the detector columns, and trimming it to the same dimensions of the original image. Then, we subtracted this wave-pattern frame from the pairwise-subtracted frame from which it was produced. In this way, a deep spectroscopic frame is obtained by combining the pairwise-subtracted, wave-pattern subtracted frames; after correcting for the telescope nodding this frame contains no detectable trace of the pickup noise, thus greatly increasing the visibility of possible spectral traces of extremely faint objects.

3. DISCUSSION

3.1. *The Spectrum of Cha I J110814.2–773649*

Examination of the deep spectroscopic frame (the combination of our 10 hr of integration) shows no hint of emission lines at the expected position of the spectrum of Cha I J110814.2–773649, while it is possible to show that the sensitivity of this frame should be sufficient to easily reveal any emission lines dominating the H -band flux. The background noise in the spectroscopic frame varies greatly depending on whether or not strong OH airglow lines are present at the corresponding wavelength. On the other hand, the spectrum of the $H = 16.83$ reference star allows us to perform an approximate flux calibration, and thus determine the number of counts that should be expected in a single line dominating the emission. In this way, we find that if the H -band flux of Cha I J110814.2–773649 were contributed by a single line with a Gaussian profile peaking at the wavelength most affected by airglow emission, its FWHM should exceed 360 \AA , so that its peak intensity integrated over the spatial profile would fall below 3 times the local background noise at that detector column. Such width would correspond to a rest-frame line width of 145 \AA for $H\alpha$ at $z = 1.5$, 110 \AA for $H\beta$ or $[\text{O III}]$ at $z = 2.3$, or 82 \AA for $[\text{O II}]$ at $z = 3.4$. For $H\alpha$ or $H\beta$ these values are about three times greater than those found in typical QSO spectra (vanden Berk et al. 2001). The discrepancy would be smaller for $\text{Ly}\alpha$, whose corresponding rest frame width would be only 27 \AA , although the redshift of that line into the H band would then imply $10.6 < z < 13.8$. We nevertheless should keep in mind that these are deliberately conservative limits that are made even more stringent (i.e., involving greater intrinsic widths) if we assume that the line peaks in a region less affected by skyglow. Similarly, such large widths greatly exceed those of the telluric OH line blends, thus implying intensities comparable to the peak intensity at wavelengths where airglow lines are absent and the background noise is thus much lower. We thus consider that our spectrum effectively excludes the possibility that the

H -band flux of Cha I J110814.2–773649 may be dominated by line emission.

In view of the nondetection of sufficiently strong emission lines to account for the H -band detection, we decided to increase the sensitivity to attempt the detection of the continuum by strongly binning the spectrum along the dispersion direction. The 1024 detector columns were thus collapsed into 20 bins. Each column contributed to the bin with a weight inversely proportional to the squared dispersion of the counts along it (excluding the regions affected by the trace of the reference star or by the artifacts that it produced when building the wave-pattern frame), so as to reduce the contribution of those wavelengths affected by the presence of sky airglow lines. The binned spectrum is shown in Figure 4, where we have indicated the position where the trace of the spectrum of Cha I 110814.2–773649 should be expected. Indeed, a slight increase of the number of counts over the background can be appreciated at precisely that position, especially on the left half of the frame corresponding to shorter wavelengths. The excess of counts is detectable over several bins and its peak along the spatial direction seems to be parallel to the trace of the spectrum of the reference star. We thus consider it as the actual detection of the spectrum of Cha I 110814.2–773649, demonstrating that the H band is indeed dominated by continuum emission and that the unusual colors of this object are due to an exotic spectral energy distribution rather than to the presence of emission lines.

3.2. The Nature of Cha I J110814.2–773649

3.2.1. An Extremely High- z Galaxy?

The existence of an object with the colors of Cha I J110814.2–773649 in exposures such as those presented here must be interpreted with caution. On the one hand, such deep images have the potential to allow detection of objects spanning a wide range of redshifts, and sampling of the rest-frame ultraviolet spectrum of objects in early evolutionary stages that are absent from the local universe; such images are thus sensitive to sources with colors widely different from those characteristic of brighter, and typically nearer objects. On the other hand, observations of fields in the JHK_S bands to a depth comparable to that of our observations are still scarce, although recent and ongoing efforts such as the deep JHK_S imaging of the Hubble Deep Field–South (HDF-S) (Labbé et al. 2003), the MS 1054-03 cluster (Franx et al. 2000), and the multiband imaging of the Chandra Deep Field–South (Renzini et al. 2003) are providing valuable information on the near-infrared colors found at such faint magnitudes. Other deep near-infrared surveys recently carried out with 8 m class telescopes, such as the Subaru Deep Field (Maihara, Iwamuro, & Tanabe 2001), have tended to use the J and K_S bands alone, because of their focus on the detection of very red objects. As a result, the framework for comparison of our results, especially concerning objects with unusual colors such as Cha I J110814.2–773649, is still rather limited. In any case, a comparison to published JHK_S data for the HDF-S over a similar field of view (Labbé et al. 2003) does confirm that the colors of Cha I J110814.2–773649 are quite unique, despite the fact that the HDF-S survey reaches down to limiting magnitudes (3σ) that are respectively 1.6 (J_S), 2.7 (H), and 2.2 mag (K_S) fainter than those of Cha I J110814.2–773649.

No objects with similar colors are detected either in deep-infrared images of the Hubble Deep Field–North (HDF-N), although the presence of an object with very atypical colors,



FIG. 4.—Combined frame containing the VLT/ISAAC spectrum of Cha I J110814.2–773649. The white trace in the upper part corresponds to the bright reference star, and the arrow marks the expected position of the trace of the spectrum of Cha I J110814.2–773649. The black stripes are artifacts of the data reduction. The spectrum ranges from $1.4\ \mu\text{m}$ (left) to $1.8\ \mu\text{m}$ (right) and is strongly binned along the dispersion direction to enable detection of the $H = 22.16$ object. See § 2.2 for a detailed explanation of the reduction process.

HDF-N J123656.3+621322 (HDFN-JD1), has been reported by Dickinson et al. (2000) in near-infrared images of that field. The object in the HDF-N is outstanding because of its very red $H-K$ color, and for being undetected at J , thus being by far the reddest object in the field in $J-H$. Although HDFN-JD1 may be considered as the opposite of Cha I J110814.2–773649 as far as $H-K$ is concerned (HDFN-JD1 being extremely red, while Cha I J110814.2–773649 is unusually blue), the large $J-H$ values are puzzling in both cases. It is interesting in this respect to consider Figure 7 of Dickinson et al. (2000), which considers the variation of the $J-H$ and

$H-K_S$ colors with redshift for a number of galaxy types modeled after the spectral energy distributions of Bruzual & Charlot (1993). The curves presented there range from a passively evolving elliptical galaxy formed at $z = 15$ to an unreddened starburst galaxy, and can be considered as bracketing the entire range of colors encountered among extragalactic objects. The bluest $H-K_S$ colors predicted by such models are produced by unreddened starbursts, reaching $H-K_S \simeq +0.2^3$ near $z = 2.5$ and $z = 5.5$. However, such redshifts are ruled out by the very blue J_S-H predicted in both cases, which are incompatible with the extremely red J_S-H of Cha I J110814.2–773649. At larger redshifts the Ly α forest enters the near infrared, progressively decreasing the flux in the J band. At $z = 8.5$ and greater the flux depletion on the blue side of the J band moves the J_S-H color above 1.4 mag, thus becoming compatible with our lower limit, while still maintaining a relatively blue $H-K_S$ at 0.35 mag. Similarly, blue $H-K_S$ colors and ever redder J_S-H colors are predicted as the starburst is shifted up to $z \simeq 11$, where Ly α enters the H band and starts reddening $H-K_S$ as well. While the error bars of our observations do not completely exclude $H-K_S = 0.35$ for Cha I J110814.2–773649 it must be recalled that, as noted in § 2.1, a foreground extinction of at least 0.2 mag, caused by dust in the Cha I cloud, pervades the field, thus reddening any background objects by at least 0.1 mag in $H-K_S$. The bluest high-redshift starbursts should thus have $H-K_S > 0.45$, which we consider hardly compatible with our measured fluxes. In summary, we consider an unreddened starburst at $8.5 < z < 11$ as a marginally consistent explanation for the unusual colors of Cha I J110814.2–773649, based on arguments similar to the ones that led Dickinson et al. (2000) to propose a $z = 12.5$ object as a possible interpretation of HDFN-JD1.

3.2.2. A Young Planetary-Mass Object?

Although an extremely high redshift object may indeed account for the spectral energy distribution of Cha I J110814.2–773649, the serendipity of its discovery and its location in the direction of a nearby star-forming region leads us to consider the alternative possibility that it may be a young, isolated planetary-mass member of Cha I. Near-infrared spectra of T dwarf–like objects are dominated by strong molecular absorption caused by CH₄, H₂O, and H₂, producing a broadband spectral energy distribution characterized by blue $J-H$ and $H-K$ colors. At the somewhat higher temperatures of L-type dwarfs, dust is present in the atmosphere in the form of clouds containing a complex mixture of metals and minerals (Burrows et al. 2001), producing extremely red colors instead. The disruption of clouds and precipitation of their condensates below the photosphere is thought to happen over a relatively narrow margin of temperatures around $T \simeq 1200$ K (Burgasser et al. 2002), marking the transition between the L and T spectral types.

The tracks overplotted in Figure 1 represent the colors and magnitudes expected for young L and T dwarf–like objects at the distance of Cha I, after the evolutionary tracks of Chabrier et al. (2000) (DUSTY models) and Baraffe et al. (2003) (COND models). The former (Fig. 1, *dashed lines*) are expected to represent L dwarf–like, dusty atmospheres, appropriate for objects hotter than $T \simeq 1200$ K, while the latter

reproduce the characteristics of cooler objects in which dust has precipitated below the photosphere. The transition temperature between the DUSTY and the COND tracks is attained at an H magnitude between 18.5 and 19.2 on the COND tracks, and between 20.5 and 21.3 on the DUSTY tracks. The magnitude intervals quoted reflect the mild age-dependence of the temperature-magnitude relationship over the 1–10 Myr range. As seen in Figure 1, both the faint H magnitude of Cha I J110814.2–773649 and its location offset blueward from the general distribution of objects in the color-magnitude diagram can be well reproduced by an extremely low mass member of the star-forming region. This is fairly independent of the assumed age, because of the broad overlap of the tracks. However, the assigned mass does depend strongly on the age, as the symbols indicating the location of objects with a given mass show. Remarkably, adopting the age that best reproduces the locations of very low mass stars and massive brown dwarfs in Cha I, which is 2 Myr, yields a mass of only $\sim 0.7M_J$ for Cha I J110814.2–773649, or about 2 Saturn masses. The spectrum of the object (Fig. 5) displays hints of a possible peak around $1.55 \mu\text{m}$ followed by a drop to near-zero emission levels at longer wavelengths, consistent with the overall spectral energy distribution of T dwarfs that also peaks at the same position. However, the extremely low signal in the spectrum makes the actual existence of the peak doubtful. It should also be pointed out that the rise near $1.8 \mu\text{m}$, if real, would have no correspondence in T dwarf spectra, thus casting doubts on this interpretation.

The agreement of the H and K_S photometry with models of very young T dwarf–like objects does not hold when we also consider the J_S-H color, which is generally close to zero in T dwarf spectra. As seen in the color-color diagram of Figure 2, while $H-K_S$ is fully within the range expected for a T dwarf–like object, the $J_S-K_S > 1.4$ of Cha I J110814.2–773649 seems characteristic of a cool L dwarf instead. In this respect, the photometric properties of Cha I J110814.2–773649 qualitatively resemble those of transition objects between the

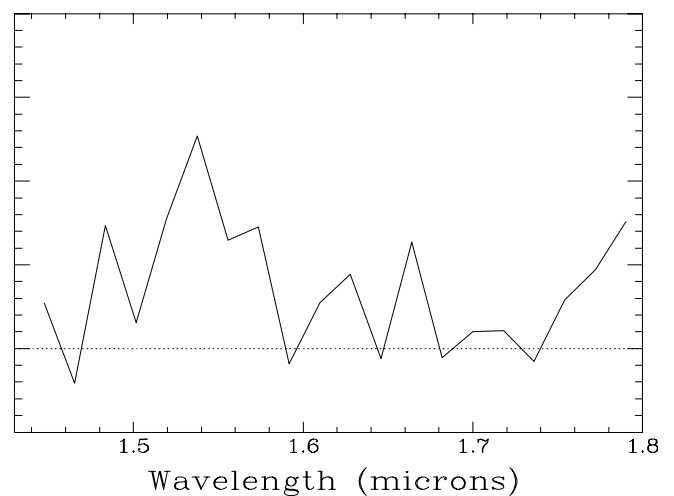


FIG. 5.—Extracted spectrum of Cha I J110814.2–773649. Relative flux calibration was achieved by finding the ratio of the object’s binned spectrum to that of the bright reference star included in the slit, and then multiplying by the ratio between a spectrum of this star and that of the B4 V star HD 94414, observed one after another at similar mass and degraded to the same resolution, and then multiplying by a $T = 17,200$ K blackbody that approximates the spectral energy distribution of HD 94414. The lower dotted line marks the zero flux level.

³ The AB magnitudes used by Dickinson et al. (2000) have been transformed into the Vega magnitudes used throughout this paper for comparison.

L and T types observed by Leggett et al. (2000), which are attributed to the persistence of dust in the atmosphere coexisting with the onset of strong CH₄ absorption in the *K* band. The sequence of colors along this transition is not well known, as it depends on factors such as the partial disruption of clouds (Burgasser et al. 2002), the composition of grains (Lodders 1999), and their size distribution, which in turn are sensitive functions of the surface gravity (Cooper et al. 2003). The low gravity of cool young planetary-mass objects, over 2 orders of magnitude lower than that of the field-evolved objects with which models have been mainly confronted so far, implies important structural differences in both the atmosphere and the layers beneath the photosphere. The lower gravity brings convection much closer to the photosphere than in evolved T dwarfs (Burrows et al. 1997), thus facilitating the presence of small grains in the atmosphere that are due to convective overshooting or turbulent diffusion (Chabrier & Baraffe 2000) at temperatures under which they would be absent in more evolved objects. All these factors might account for the maintenance of hybrid features such as L dwarf-like reddening at *J_S-H* and T dwarf-like blueing at *H-K_S* at even lower temperatures and luminosities in young planetary-mass objects, accounting for the observed colors of Cha I J110814.2–773649 despite a brightness that is well below that predicted for a young early-T object. At this point this is a very speculative explanation unsupported by proper modeling, but the identification of such hybrid features as being common among other young very low mass objects could lend support to it.

It is interesting in this respect to compare Cha I J110814.2–773649 with S Ori 70, a confirmed T dwarf-like object recently discovered by Zapatero Osorio et al. (2002) in the direction of the σ Ori association. The membership of S Ori 70 in σ Ori, and therefore its youth, is considered likely by these authors, based on both probabilistic arguments derived from the actual density of similar objects in the field, and on fits to theoretical spectra with different surface gravities, which tend to give a better match for low surface gravity values. This has been recently confirmed by Martín & Zapatero Osorio (2003), based on mid-resolution infrared spectroscopy. This object is considerably brighter than Cha I J110814.2–773649, despite the distance to σ Ori being over twice that to Cha I: if both are members of their respective star-forming regions, the difference in absolute *H* magnitudes is about 3.5 mag. Interestingly, S Ori 70 also has unusual colors for a T dwarf-like object, albeit in a different sense to Cha I J110814.2–773649: while the *J-H* color of S Ori 70 is very blue and consistent with those of field T dwarfs, its *H-K* color is unusually red when compared to an object of this class (Dahn et al. 2002; Leggett et al. 2002), as well as to the best-fitting theoretical models. Moreover, its brightness places it between 1 and 2 mag above the sequence predicted by models in color-magnitude diagrams for objects of the same color. The spectroscopic confirmation of S Ori 70 as a T dwarf-like object, and its likely membership in σ Ori, is thus a caution to be aware of the diversity found among otherwise similar objects of this kind, and the limited reliance that must be placed on the models.

4. CONCLUSIONS

In this paper we have reported the discovery, with the ESO Very Large Telescope, of an object in the direction of the Cha I star-forming region, Cha I J110814.2–773649, characterized by its unusual near-infrared colors. The object is faint

($H = 22.16^{+0.21}_{-0.17}$), very red in *J_S-H* ($2.00^{+\infty}_{-0.62}$), and very blue in *H-K_S* ($-0.01^{+0.26}_{-0.24}$). A 10 hr *H*-band spectrum demonstrates that the colors are not due to the presence of strong emission lines in the *H* band, and actually reveals the continuum of the object.

We consider two possible interpretations for Cha I J110814.2–773649. In the first interpretation, corresponding to a very high redshift object, a marginally acceptable match to the colors is found by assuming that Cha I J110814.2–773649 is an unreddened starburst, turned into a *J*-band dropout by an extremely high redshift ($8.5 < z < 11$) that makes the Ly α forest penetrate well into the *J* band. Other spectral energy distributions at different, lower redshifts cannot simultaneously reproduce both the red *J_S-H* and the blue *H-K_S* colors. The very high redshift implied by this explanation, which greatly exceeds that of any spectroscopically confirmed source known so far, and the important quantitative difference between the bluest *H-K_S* color allowed by the models and the observed color makes us consider it quite unlikely.

The second explanation, motivated by the location of Cha I J110814.2–773649 in the general direction of the Chamaeleon I cloud, is that it may be an actual very low mass member of that region. Taken together, the *H-K_S* color and the *H* magnitude are consistent with the model predictions for a planetary-mass object of roughly 0.7 Jupiter masses with an age of 2 Myr, or slightly above $1M_J$ if it is 5 Myr old. However, this explanation does not seem consistent with the very red *J_S-H* color implied by the marginal detection at *J_S*, which models predict only for the coolest dusty atmospheres. We speculate that Cha I J110814.2–773649 might be an object with spectral features that are a hybrid between those of L and T dwarfs, displaying both a dusty atmosphere that reddens *J_S-H* while at the same time having strong CH₄ bands that make *H-K_S* blue, with the coexistence of both features being possible due to the low surface gravity of such a young object.

Both possible explanations are quite exciting: the first would imply that Cha I J110814.2–773649 is a record-breaking high-redshift object, while the second would make it the least massive compact object so far identified outside the solar system. It is thus tantalizing to be unable to distinguish between these two radically different possibilities with the data currently at hand, and it must be kept in mind that the subsisting photometric uncertainties do not completely exclude other less exotic possibilities. Further ground-based spectroscopy will demand great amounts of integration time at the largest telescopes, and detection at longer wavelengths must wait for the next generation of space-borne infrared observatories (Burrows et al. 2001). However, new observations of Cha I 110814.2–773649 and other possible new, young, isolated planetary-mass objects with currently available means are important. A better determination of the unusual colors of Cha I 110814.2–773649 and monitoring for variability are obvious follow-up tasks, while astrometry, which could confirm kinematical membership over a timescale of 5–10 yr, would address the origin of Cha I 110814.2–773649 as either an isolated object or as a former planet expelled from its parent stellar system (de la Fuente Marcos & de la Fuente Marcos 1999; Reipurth & Clarke 2001). Finally, new deep searches in star-forming regions will tell us if young, isolated planetary-mass objects are a common outcome of stellar- and planetary-system formation, or rather a rarity among astrophysical objects.

We are very pleased to thank Adam Burrows for providing details on his model calculations and for a critical reading of an earlier version of this manuscript. France Allard and Isabelle Baraffe are thanked for useful remarks on the validity of the Baraffe et al. (2003) model predictions at the very young ages of relevance here. Insightful comments by the

referee, Phil Lucas, as well as a second anonymous referee, and the editor, James Liebert, helped improve this paper in both content and presentation. Last but not least, the excellent support received from the Paranal Science Operations staff during our VLT observations in 2000 and 2001 is warmly appreciated.

REFERENCES

- Baraffe, I., Chabrier, G., Barman, T. S., Allard, F., & Hauschildt, P. H. 2003, *A&A*, 402, 701
- Bessell, M. S., & Brett, J. M. 1988, *PASP*, 100, 1134
- Boss, A. P. 2001, *ApJ*, 551, L167
- Bruzual, G., & Charlot, S. 1993, *ApJ*, 405, 538
- Burgasser, A. J., Marley, M. S., Ackerman, A. S., Saumon, D., Lodders, K., Dahn, C. C., Harris, H. C., & Kirkpatrick, J. D. 2002, *ApJ*, 571, L151
- Burgasser, A. J., et al. 1999, *ApJ*, 522, L65
- Burrows, A., Hubbard, W. B., Lunine, J. I., & Liebert, J. 2001, *Rev. Mod. Phys.*, 73, 719
- Burrows, A., et al. 1997, *ApJ*, 491, 856
- Chabrier, G., & Baraffe, I. 2000, *ARA&A*, 38, 337
- Chabrier, G., Baraffe, I., Allard, F., & Hauschildt, P. 2000, *ApJ*, 542, 464
- Comerón, F., Neuhäuser, R., & Kaas, A. A. 2000, *A&A*, 359, 269
- Comerón, F., Reipurth, B., Henry, A., & Fernández, M. 2003, *A&A*, in press
- Cooper, C. S., Sudarsky, D., Milsom, J. A., Lunine, J. I., & Burrows, A. 2003, *ApJ*, 586, 1320
- Dahn, C. C., et al. 2002, *AJ*, 124, 1170
- de la Fuente Marcos, C., & de la Fuente Marcos, R. 1999, *NewA*, 4, 21
- Dickinson, M., et al. 2000, *ApJ*, 531, 624
- Franx, M., et al. 2000, *Messenger*, 99, 20
- Kirkpatrick, J. D., et al. 1999, *ApJ*, 519, 802
- Labbé, I., et al. 2003, *AJ*, 125, 1107
- Leggett, S. K., et al. 2000, *ApJ*, 536, L35
- . 2002, *ApJ*, 564, 452
- Lodders, K. 1999, *ApJ*, 519, 793
- Lucas, P. W., & Roche, P. F. 2000, *MNRAS*, 314, 858
- Lucas, P. W., Roche, P. F., Allard, F., & Hauschildt, P. H. 2001, *MNRAS*, 326, 695
- Maihara, T., Iwamuro, F., & Tanabe, H. 2001, *PASJ*, 53, 25
- Martín, E. L., & Zapatero Osorio, M. R. 2003, *ApJ*, 593, L113
- Persson, S. E., Murphy, D. C., Krzeminsky, W., Roth, M., & Rieke, M. J. 1998, *AJ*, 116, 2475
- Reipurth, B., & Clarke, C. J. 2001, *AJ*, 122, 432
- Renzini, A., et al. 2003, in *The Mass of Galaxies at Low and High Redshifts*, ed. R. Bender & A. Renzini (New York: Springer), 332
- Saumon, D., et al. 1996, *ApJ*, 460, 993
- Stetson, P. B. 1987, *PASP*, 99, 191
- Tinney, C. G., ed. 1995, *The Bottom of the Main Sequence—and Beyond* (Heidelberg: Springer)
- vanden Berk, D. E., et al. 2001, *AJ*, 122, 549
- Wichmann, R., Bastian, U., Krautter, J., Jankovics, I., & Ruciński, S. M. 1998, *MNRAS*, 301, L39
- Zapatero Osorio, M. R., Béjar, V. J. S., Martín, E. L., Rebolo, R., Barrado y Navascués, D., Bailer-Jones, C. A. L., & Mundt, R. 2000, *Science*, 290, 103
- Zapatero Osorio, M. R., Béjar, V. J. S., Martín, E. L., Rebolo, R., Barrado y Navascués, D., Mundt, R., Eisloffel, J., & Caballero, J. A. 2002, *ApJ*, 578, 536
- Zapatero Osorio, M. R., Béjar, V. J. S., Rebolo, R., Martín, E. L., & Basri, G. 1999, *ApJ*, 524, L115